Available online at www.sciencedirect.com
ScienceDirect
Materials Chemistry and Physics 103 (2007) 190–194
MATERIALS CHEMISTRY AND PHYSICS
www.elsevier.com/locate/matchemphys

Growth and optical properties of ZnO nanostructures by vapor transport process

Y.H. Tong [a,b,c], Y.C. Liu [c,*], L. Dong [d], L.X. Lu [e], D.X. Zhao [a], J.Y. Zhang [a], Y.M. Lu [a], D.Z. Shen [a], X.W. Fan [a]

[a] *Key Laboratory of Excited State Process, Changchun Institute of Optics, Fine Mechanics and Physics, Chinese Academy of Sciences, Changchun 130033, PR China*
[b] *Graduate School of Chinese Academy of Science, Beijing 100039, PR China*
[c] *Center for Advanced Opto-Electronic Functional Material Research, Northeast Normal University, Changchun 130024, PR China*
[d] *School of Materials Science and Engineering, Zhengzhou University, Zhengzhou 450052, PR China*
[e] *School of Science, Hebei University of Technology, Tianjin 300130, PR China*

Received 12 May 2006; accepted 13 February 2007

Abstract

ZnO nanorods and ZnO nanotubes have been fabricated by thermally evaporating the metal Zn powder. The ZnO nanorod obtained on the ITO substrate located above the Zn source has the uneven diameter with the abrupt change in its middle, which may originate from the decrease of the Zn vapor in the system. The ZnO nanotubes with the rough surfaces were obtained in the upstream region. The negative thermal quenching of the photoluminescence can be observed in the ZnO nanotubes. This is related with the abundant surface/interface defects which can introduce a large number of middle states in the band gap. According to Shibata's model, the activation energy of the electrons from the middle states to the initial states can be obtained by fitting the experimental data of the temperature dependence of the ultraviolet photoluminescence intensity. The fitting energy values are as high as ~100 meV, which may be responsible for the negative thermal quenching in a high-temperature range from 163.5 to 205.6 K.

Keywords: ZnO; Surfaces/interfaces; Optical properties

1. Introduction

Zinc oxide (ZnO), due to its wide band gap (3.37 eV), high exciton binding energy (60 meV), low cost, excellent thermal and chemical stability, have been extensively studied in many fields such as ultraviolet laser diodes, solar cells, photocatalyst and transparent conductive films. Since Yang and co-workers reported room temperature ultraviolet (UV) lasing in the ZnO nanowire arrays at a very low optical pumping threshold (40 kW cm^{-2}) [1], one-dimensional (1D) ZnO nanostructures, including nanowires [2], nanobelts [3], nanoneedles [4] and nanotubes [5], have been attracting worldwide attention due to their novel properties and potential applications in nanoscale optoelectronics. The growth mechanisms of the ZnO nanostructures obtained in different conditions have been extensively investigated in order to manipulate their growth, morphology, properties and applications. Recently, based on these 1D ZnO nanostructures, transistors [6], optical waveguide [7], solar cells [8], ultraviolet photodetectors and optical switches [9], have been fabricated and the device performances have been investigated.

Because of the small size and large surface area-to-volume ratio, the surface effect is an important issue which seriously influences the properties of the ZnO nanostructures and the performances of the 1D ZnO-based devices. Photoluminescence (PL) investigation provides a simple and sensitive method to characterize the surfaces of materials [10]. When the above-bandgap light is incident on a material, for example, the ZnO material, the incident light is mainly absorbed by the surface and hence the PL often originates near the surface of the material. As a result, the PL not only can reflect the bandgap and exciton levels, radiative and nonradiative recombination processes,

* Corresponding author. Tel.: +86 431 5099168; fax: +86 431 5684009.
E-mail address: ycliu@nenu.edu.cn (Y.C. Liu).

0254-0584/$ – see front matter © 2007 Elsevier B.V. All rights reserved.
doi:10.1016/j.matchemphys.2007.02.015

but also can provide the information of the surface and interface states. Therefore, it is a crucial issue to study the PL properties of the ZnO nanostructures for the practical applications.

In this paper, we fabricated ZnO nanorods and nanotubes by the vapor transport process. Their growth mechanisms were investigated. The PL properties of the ZnO nanotubes were studied in detail. The visible emission band is broadened compared with that of the bulk ZnO. The temperature dependence of the PL intensity is quite different from the most reported results.

2. Experimental details

The growth was performed in a horizontal tube furnace. The plasma treated ITO glasses were used as substrates. A quartz boat located with the pure Zn powder was placed into the center of the horizontal tube furnace. One glass substrate was located above the Zn source at a vertical distance of ~2 mm with its conductive side facing downward. The other substrate was placed upstream ~15 cm away from the Zn source. N_2 was introduced to the chamber as the carrier gas and the system was evacuated by a mechanical pump. No oxygen flow was intentionally introduced. The furnace was heated to 500 °C from room temperature for 40 min and then the temperature was maintained at 500 °C for 40 min. Finally, the furnace was cooled to room temperature. The ITO substrate located above the Zn source was covered with a semitransparent film and the other located in the upstream region was covered with a white film.

The structures of the products were analyzed by X-ray diffraction (XRD; Rigaku D/max-rA). The morphology was examined with field-emission scanning electron microscope (FESEM; Hitachi S-4300). The PL spectra were carried out with a He–Cd laser at 325 nm. The optical measurements were performed using a LABRAM-UV Raman microspectrometer (Jobin Yvon).

3. Results and discussion

Fig. 1 shows the XRD patterns of the two samples. Only the (0 0 2) diffraction peak of ZnO can be observed for the product obtained on the ITO substrate located above the Zn source, indicating the amount of the resident and/or leaky oxygen in the reaction system is large enough to oxidize Zn to obtain the pure ZnO with hexagonal wurtzite structure at the center of the furnace. Fig. 1b corresponds to the sample obtained in the upstream region. Besides ZnO (1 0 0) and (1 0 1) peaks, the Zn (1 1 2) and (0 0 6) diffraction peaks can also be observed. This indicates that the Zn cannot be fully oxidized in the lower temperature region away from the center of the tube furnace.

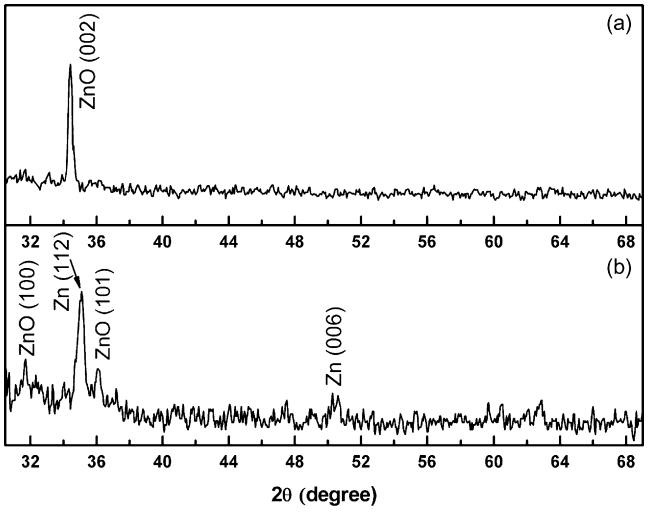

Fig. 1. XRD spectra of ZnO nanostructures: (a) obtained above the Zn source and (b) obtained in the upstream region.

Fig. 2a shows that the well arrayed 1D ZnO nanorods can be obtained on the ITO substrate located above the Zn source. This is in agreement with the XRD result which indicates the preferred growth of the ZnO nanostructures. The inset in Fig. 2a shows that the diameter of the ZnO nanorod has an abrupt change in the middle. The similar characteristic can be found in the previously reported ZnO nanostructures. Wang et al. fabricated ZnO nanopenciles with sharp tips by the two-step pressure control [11]. The sudden decrease in the working pressure can lead to the shortage of the source vapor and hence causes the abrupt change in diameter along [0 0 0 1] direction. Tseng et al. have proposed that adjusting the vapor flux of the zinc source can control the diameter of ZnO nanorods [12]. Combined with their results, we assume that the abrupt change of the diameter in the middle of the single ZnO nanostructure may be also related with the change of the Zn vapor. The melting point of Zn is 419 °C, and hence the Zn can be evaporated in the process of elevating temperature. At the same time, the surface of the Zn powder can also be gradually oxidized. With the increasing temperature, the amount of the oxidized Zn increases, which may result in

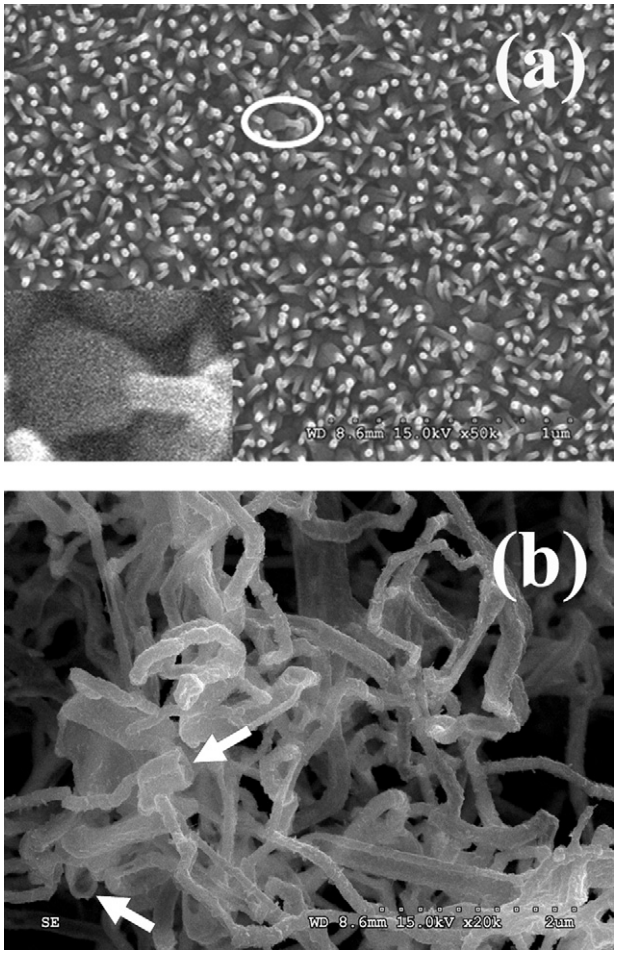

Fig. 2. SEM images of ZnO nanostructures: (a) ZnO nanorods obtained above the Zn source. The inset is the single nanorod corresponding to the region as marked by the circle. (b) ZnO nanotubes obtained in the upstream region.

the decrease of the Zn vapor in the system. When the temperature reaches a certain value, the oxidization and evaporation processes of the Zn source may attain equilibrium. In this case, a small amount of Zn was evaporated out resulting in the thinner nanorods grown on the top of the nanorods with the bigger diameters.

Fig. 2b shows the SEM image of the white product obtained in the upstream region. It is interesting that the hollow structure can be observed from the end of the single nanostructure (marked with arrow heads), indicating the formation of the tubular structure. Based on the synthetic process and the experimental results, the possible mechanism is as follows. Before the temperature reaches 500 °C, the Zn vapor is diffused to a lower temperature region, where the Zn vapor condenses forming the Zn nanowires. With the increase of the temperature at the center of the furnace, the temperature at the deposition region also increases. In this case, the higher temperature makes that the residual and/or leaky oxygen in the system can oxidize the Zn nanowires. Moreover, the surface of the Zn nanowire will be first oxidized to form the ZnO shell layer, resulting in the white product observed on the substrate. The formation of the ZnO shell layer will slow down the oxidation process of the Zn in the inner layer. With the decrease of the temperature in the cooling process, the residual Zn in the ZnO cell layer can no longer be evaporated out when the temperature in the deposition region decreases below the melting point of the Zn. So the diffraction peaks related with the metal Zn are also observed in the XRD spectrum, as shown in Fig. 1. The oxidation of the Zn nanowires and the evaporation of the metal Zn in the ZnO cell layer result in the formation of the tubular structure.

As mentioned above, the surface is an important feature for the nanostructures and the PL investigations can be used to characterize the surfaces/interfaces of the nanostructures. The PL peak positions can be analyzed to determine the bandgap and defect energy levels, and the temperature dependence of the PL intensity can reflect the carrier population on different energy states. Here, we select the ZnO nanotubes to study the optical properties of the ZnO nanomaterials in detail. The room temperature PL spectrum of ZnO nanotubes is shown in Fig. 3. The ultraviolet (UV) peak originates from the exciton recombination. Compared with bulk ZnO, the visible emission is broadened and it can be deconvoluted into two bands centered at about 520 and 600 nm, respectively (a serious of peaks superimposed on the visible emission band originate from the measurement equipment). The green band at about 520 nm, which is frequently observed in ZnO material, is generally assumed to be related with oxygen deficiency [13,14]. The orange band at about 600 nm may be associated with the oxygen interstitial defects [15,16]. Although the nature of the visible emission remains controversial, it is widely acknowledged that it is related to the surface defects. Our previous results also proved that the broadening of visible emission band is closely related with the surface defect introduced energy band [17]. Therefore, the broadening visible emission implies the rich surface/interface defects existing in ZnO nanotubes.

Fig. 4 shows the UV PL spectra of the ZnO nanotubes at different temperatures ranging from 163.5 to 301.3 K. The inset

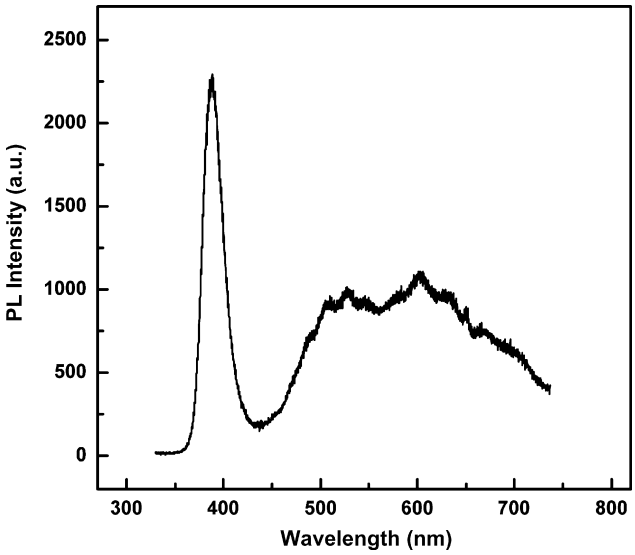

Fig. 3. Room temperature PL spectrum of ZnO nanotubes.

is a typical PL spectrum measured at 163.5 K. A weak free exciton emission (labeled with E_{ex}) can be observed at around 3.327 eV. The dominant peak at 3.297 eV, which is 30 meV lower than the E_{ex} peak, can be assigned to the acceptor-bound exciton (labeled with B_{ex}) [18]. Three peaks in the lower-energy side at about 3.325, 3.153 and 3.081 eV, are clearly observed and show the energy separation of 72 meV, which is consistent with the theoretical value for the ZnO longitudinal optical (LO) phonon replica energy. Therefore, they can be attributed to first-, second- and third-order LO phonon replicas of the B_{ex}, respectively. The PL peak shifts towards lower energy with the increasing temperature resulting from the decrease in the band gap. The emission intensity has an anomalous feature which first increases at the lower temperature range and then begins to decrease at 205.6 K. The B_{ex} peak and its first- and

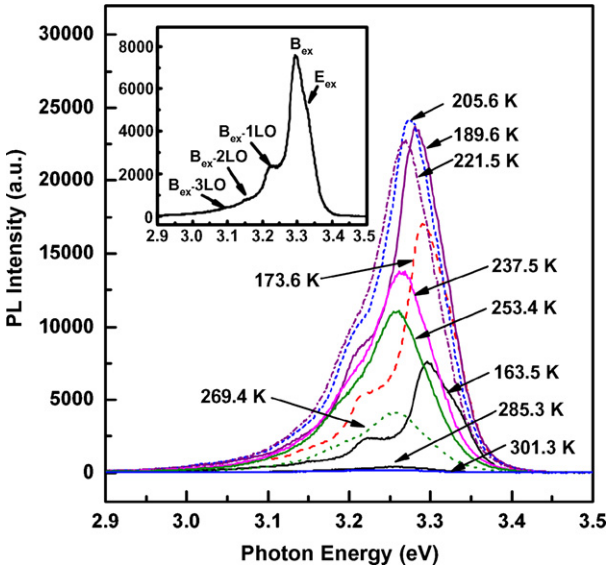

Fig. 4. UV PL spectra of the ZnO nanotubes at different temperatures ranging from 163.5 to 301.3 K. The inset is an enlarged PL spectrum measured at 163.5 K.

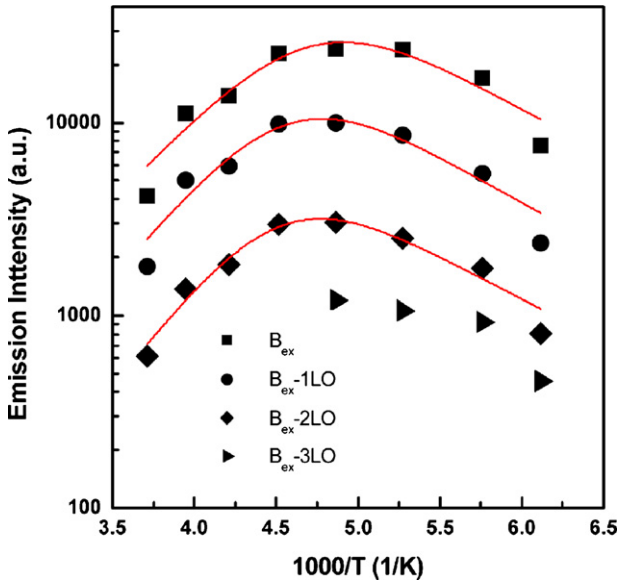

Fig. 5. PL intensity of the UV emission as a function of the temperature ranging from 163.5 to 269.4 K for the ZnO nanotubes. The solid curves represent theoretical fitting results.

second-order phonon replicas can be observed till 269.4 K. The temperature dependences of the PL intensity for the B_{ex} and the three-order phonon replicas are clearly shown in Fig. 5 by scatter plots.

Generally, the PL intensity decreases monotonically with the increasing temperature due to the increase in the nonradiative recombination probability of electrons and holes with the increasing temperature. The anomalous phenomenon that the PL intensity increases with the increasing temperature, i.e., the negative thermal quenching of the PL, has been observed in GaAs, ZnS and ZnO materials [19,20]. Our previous work has also indicated that the abnormal temperature dependence of the PL intensity could be observed in ZnO nanocrystal thin films [21], ZnO microrods [22] and ZnO nanorods [23]. Obviously, the anomalous PL phenomenon is frequently found in the ZnO nanostructures. Shibata proposed that the negative thermal quenching originated from the thermal excitation of the electrons to the initial states (excited states) of the PL transition from the intermediated states [19]. These experimental and theoretical results imply that the plural energy states may be related with the special structures. As we know, there are a large number of defects, especially surface and interface defects, existing in nanostructures. Abundant surface/interface defects in the ZnO nanostructures will introduce a number of middle states to trap carriers. When the energy separation between the initial state and some of the middle states is comparable to the temperature of the system, the thermal excitation of electrons from the latter states to the former states is not negligible. Considering that the PL intensity is proportional to the number of electrons in initial states, the temperature dependences of the PL intensity can be fitted by the formula [19]:

$$I(T) = I(0)\frac{1 + D\exp(-E_q/k_BT)}{1 + C\exp(-E_j/k_BT)}$$

Table 1
The values of the parameters E_q and E_j obtained by fitting the theoretical formula

	E_q (meV)	E_j (meV)
B_{ex}	102	278
B_{ex}-1LO	105	303
B_{ex}-2LO	99	310

where E_q is the activation energy of the electrons from the intermediated states to the initial states and E_j is the activation energy for the nonradiative recombination process. The fitting results are shown in Fig. 5 as the solid curve for comparison with the experimentally obtained results. The values of the parameters E_q and E_j which give the best fitting to the experimental results are shown in Table 1. The obtained E_q values have quite high energy, which may be responsible for the negative thermal quenching in a high-temperature range from 163.5 to 205.6 K.

4. Conclusion

We have fabricated the ZnO nanostructures on the ITO substrates by thermally evaporating the metal Zn. The single nanorod obtained above Zn source has an abrupt change in diameter along the growth direction, which is likely due to the decrease of the Zn vapor. The formation of nanotubes in the upstream region is possibly attributed to the evaporation of the Zn in the ZnO cell layer. The room temperature PL spectrum of the ZnO nanotubes shows the exciton emission and the defect-related visible emission. The anomalous temperature dependences of the UV PL intensity originate from the thermal excitation of carriers in defect states.

Acknowledgements

This work is supported by the Key Project of National Natural Science Foundation of China under Grant No. 60336020, the National Natural Science Foundation of China under Grant Nos. 60278031, 60376009, 60506014, 50402016 and 60501025 and the Innovation Project of Chinese Academy of Sciences.

References

[1] M.H. Huang, S. Mao, H. Feick, H. Yan, Y. Wu, H. Kind, E. Weber, R. Russo, P. Yang, Science 292 (2001) 1897.
[2] C. Xu, K. Rho, J. Chun, D. Kim, Appl. Phys. Lett. 87 (2005) 253104.
[3] Z.W. Pan, Z.R. Dai, Z.L. Wang, Science 291 (2001) 1947.
[4] B. Liu, H.C. Zeng, Langmuir 20 (2004) 4196.
[5] J.S. Jeong, J.Y. Lee, J.H. Cho, H.J. Cho, H.J. Suh, C.J. Lee, Chem. Mater. 17 (2005) 2752.
[6] J. Goldberger, D.J. Sirbuly, M. Law, P. Yang, J. Phys. Chem. B 109 (2005) 9.
[7] M. Law, D.J. Sirbuly, J.C. Johnson, J. Goldberger, R.J. Saykally, P. Yang, Science 305 (2004) 1269.
[8] M. Law, L.E. Greene, J.C. Johnson, R. Saykally, P. Yang, Nat. Mater. 4 (2005) 455.
[9] H. Kind, H. Yan, B. Messer, M. Law, P. Yang, Adv. Mater. 14 (2002) 158.
[10] T.H. Gfroerer, in: R.A. Meyers (Ed.), Encyclopedia of Analytical Chemistry, Wiley, Chichester, 2000, pp. 9209–9211.
[11] R.C. Wang, C.P. Liu, J.L. Huang, S.J. Chen, Y.K. Tseng, S.C. Kung, Appl. Phys. Lett. 87 (2005) 013110.

[12] Y. Tseng, C. Huang, H. Cheng, I. Lin, K. Liu, I. Chen, Adv. Func. Mater. 13 (2003) 811.
[13] A. van Dijken, E.A. Meulenkamp, D. Vanmaekelbergh, A. Meijerink, J. Phys. Chem. B 104 (2000) 1715.
[14] S. Monticone, R. Tufeu, A.V. Kanaev, J. Phys. Chem. B 102 (1998) 2854.
[15] H.S. Kang, J.S. Kang, J.W. Kim, S.Y. Lee, Phys. Status Solidi (c) 1 (2004) 2550.
[16] S.A. Studenikin, N. Golego, M. Cocivera, J. Appl. Phys. 84 (1998) 2287.
[17] Y.H. Tong, Y.C. Liu, C.L. Shao, R. Mu, Appl. Phys. Lett. 88 (2006) 123111.
[18] U. Ozgur, Y.I. Alivov, C. Liu, A. Teke, M.A. Reshchikov, S. Dogan, V. Avrutin, S.-J. Cho, H. Morkoc, J. Appl. Phys. 98 (2005) 041301.
[19] H. Shibata, Jpn. J. Appl. Phys. 37 (1998) 550.
[20] H. Shibata, M. Watanabe, M. Sakai, K. Oka, P. Fons, K. Iwata, A. Yamada, K. Matsubara, K. Sakurai, H. Tampo, K. Nakahara, S. Niki, Phys. Status Solidi (c) 1 (2004) 872.
[21] S.J. Chen, Y.C. Liu, H. Jiang, Y.M. Lu, J.Y. Zhang, D.Z. Shen, X.W. Fan, J. Cryst. Growth 285 (2005) 24.
[22] Y.L. Liu, Y.C. Liu, W. Feng, J.Y. Zhang, Y.M. Lu, D.Z. Shen, X.W. Fan, D.J. Wang, Q.D. Zhao, J. Chem. Phys. 122 (2005) 174703.
[23] Y.W. Chen, Y.C. Liu, S.X. Lu, C.S. Xu, C.L. Shao, C. Wang, J.Y. Zhang, Y.M. Lu, D.Z. Shen, X.W. Fan, J. Chem. Phys. 123 (2005) 134701.